Biochimica et Biophysica Acta 1828 (2013) 2319–2327

Contents lists available at SciVerse ScienceDirect

Biochimica et Biophysica Acta

journal homepage: www.elsevier.com/locate/bbamem

Review

Coordination to divalent cations by calcium-binding proteins studied by FTIR spectroscopy☆

Masayuki Nara [a,*], Hisayuki Morii [b], Masaru Tanokura [c]

[a] Laboratory of Chemistry, College of Liberal Arts and Sciences, Tokyo Medical and Dental University, Chiba 272-0827, Japan
[b] National Institute of Advanced Industrial Science and Technology (AIST), Ibaraki, Japan
[c] Department of Applied Biological Chemistry, Graduate School of Agricultural and Life Sciences, University of Tokyo, Bunkyo, Tokyo, Japan

ARTICLE INFO

Article history:
Received 17 October 2012
Received in revised form 15 November 2012
Accepted 17 November 2012
Available online 29 November 2012

Keywords:
FTIR spectroscopy
COO^- group
Calcium binding protein
Coordination structure

ABSTRACT

We review the Fourier-transform infrared (FTIR) spectroscopy of side-chain COO^- groups of Ca^{2+}-binding proteins: parvalbumins, bovine calmodulin, akazara scallop troponin C and related calcium binding proteins and peptide analogues. The COO^- stretching vibration modes can be used to identify the coordination modes of COO^- groups of Ca^{2+}-binding proteins to metal ions: bidentate, unidentate, and pseudo-bridging. FTIR spectroscopy demonstrates that the coordination structure of Mg^{2+} is distinctly different from that of Ca^{2+} in the Ca^{2+}-binding site in solution. The interpretation of COO^- stretches is ensured on the basis of the spectra of calcium-binding peptide analogues. The implication of COO^- stretches is discussed for Ca^{2+}-binding proteins. This article is part of a Special Issue entitled: FTIR in membrane proteins and peptide studies.

Contents

1. Introduction

Fourier-transform infrared spectroscopy (FTIR) is a useful method for investigating protein structures [1–8]. Among the infrared bands created by the peptide group, the amide-I and amide-I′ bands have been the most widely used in studies of protein secondary structures in H_2O and D_2O solutions, respectively. The amide-I mode consists mainly of the C O stretch of the peptide group (mixed with the N–H bend and the C–N stretch) and gives rise to a strong infrared band in the region of 1700–1600 cm^{-1}. The amide-I′ mode also consists mainly of the C O stretch of the peptide group, but the band position of amide-I′ mode is very slightly downshifted due to the secondary order of perturbation by the HD exchange at NH bond of the main chain. The development of FTIR spectroscopy made it possible to enhance the resolution of broad infrared bands by techniques such as Fourier self-deconvolution [9–11], second-derivative, curve-fitting, difference calculation and two-dimensional correlation analysis [12–14]. Originally, the relationship between the positions of the amide-I band obtained by using Fourier self-deconvolution and curve-fitting and the type of secondary structure was investigated experimentally for model peptides and proteins of known three-dimensional structure by Byler and Susi [3]. The general empirical rule in the infrared study of proteins is to assign the individual amide-I bands resolved by resolution-enhancement techniques to representative secondary structures such as α-helix, β-sheet, β-turn and so on [1–8]. In particular, to understand the secondary structures of proteins

Abbreviations: Parv(s), parvalbumin(s); CaM, calmodulin; TnC, troponin C

☆ This article is part of a Special Issue entitled: FTIR in membrane proteins and peptide studies.

* Corresponding author. Tel.: +81 47 300 7122; fax: +81 47 300 7100.
E-mail address: nara.las@tmd.ac.jp (M. Nara).

0005-2736/$ – see front matter © 2012 Elsevier B.V. All rights reserved.
http://dx.doi.org/10.1016/j.bbamem.2012.11.025

qualitatively, second-derivative calculation has been widely and conveniently applied to the FTIR spectra or FTIR attenuated total reflection (ATR) spectra of proteins, after eliminating the contribution of solvent (H_2O or D_2O buffer) by a subtraction procedure.

FTIR spectroscopy also has potential in the study of protein side-chains such as aromatic rings, $-COO^-$, $-OH$, $-SH$, $-CH_3$, $-CH_2-$ and so on, to elucidate the mechanisms underlying protein reactions [7,8,15]. Wright and Vanderkooi indicated that FTIR profiles for 20 amino acids and their metabolites are sufficiently characteristic so that FTIR can be used to monitor enzymatic reactions involving amino acids [15]. Barth has reviewed the infrared absorption of amino acid side chains of proteins in H_2O and D_2O in detail [7,8]. In this review, we focus on the metal coordination of the side chain COO^- groups of Glu and Asp on Ca^{2+}-binding proteins, which plays an important role in Ca^{2+}-mediated functions [16–27].

2. Implication of infrared COO^- stretches

The carboxylate (COO^-) groups can coordinate to metal ions in four modes (Fig. 1): 'unidentate' (or 'monodentate'), 'bidentate' (or 'chelating'), 'bridging' (or 'bridging bidentate') and 'pseudo-bridging' modes [28,29]. When a metal ion interacts with only one oxygen atom of a COO^- group, the coordination structure is regarded as unidentate. In the bidentate coordination mode, the metal ion interacts equally with the two oxygen atoms of a COO^- group. In the bridging coordination mode, one metal ion binds to one of the two oxygens in a COO^- group and another metal ion to the other oxygen atom. As a special case of the bridging mode, the pseudo-bridging coordination mode features a water molecule replacing one of the two ligands in the bridging coordination. Extensive infrared studies have been done on the relationship between COO^- stretching frequencies and coordination types [28,30]. Deacon and Phillips [28] have found a general tendency in the relationship between $\Delta\nu_{a-s}$ (frequency separation between the COO^- antisymmetric and symmetric stretching vibrations) and the coordination types of the COO^- group to metal ions by examining the structures and vibrational frequencies of a number of acetate salts in the solid state. The frequency of the COO^- antisymmetric stretch of the unidentate species is higher than that of the ionic (metal-free) species, which is in turn higher than that of the bidentate species. The reverse is the case for the COO^- symmetric stretch. As a result, the $\Delta\nu_{a-s}$ values for unidentate, bridging, bidentate and ionic species are in the following order:

$$\Delta\nu_{a-s}(\text{unidentate}) > \Delta\nu_{a-s}(\text{ionic}) \sim \Delta\nu_{a-s}(\text{bridging}) > \Delta\nu_{a-s}(\text{bidentate}),$$

where $\Delta\nu_{a-s}$ (ionic) is approximately 160–170 cm^{-1}. *Ab initio* molecular orbital calculation ($HF/6-31+G^{**}$) has revealed that the correlation is related to changes in the CO bond length and the OCO angle [31]. An equation for the relationship between the structure of the COO^- group and the value of $\Delta\nu_{a-s}$ (in cm^{-1}) is given as

$$\Delta\nu_{a-s} = 1818.1\delta r + 16.47(\theta_{OCO} - 120) + 66.8,$$

where δr is the difference between the two CO bond lengths (in Å) and θ_{OCO} is the OCO angle (in degrees). This equation suggests that the variation of 0.01 Å in δr or 1° in θ_{OCO} gives rise to a change of 16–18 cm^{-1} in the value of $\Delta\nu_{a-s}$. Dudev and Lim have evaluated vibrational frequencies and absolute intensities of the COO^- stretches by using density functional theory (DFT) calculation and suggested that IR band intensities may be used to help interpret the IR spectra of protein binding sites in the metal-free and metal-bound states [32].

The empirical rule described above can be applied to other compounds, such as amino acids (glutamic and aspartic) and ethylenediaminetetraacetic acid (EDTA), although the value $\Delta\nu_{a-s}$ (ionic) depends on the compound. When we apply this empirical rule to the side-chain COO^- groups contained in a protein in solution, we see that the COO^- group, which binds to M^{2+} (bicationic metal ion) in the unidentate coordination mode in the solid state, probably contacts water molecules in aqueous solution and may become a 'pseudo-bridging' coordination mode. This is applicable to [$EDTA^{4-}$–Ca^{2+}] complex in aqueous solution [20] and most of the side chain COO^- groups in the unidentate coordination mode in Ca^{2+}-binding proteins. As a result of the coordination of the COO^- groups to Ca^{2+} in the pseudo-bridging mode, the intensity of the COO^- antisymmetric stretching band becomes stronger by the binding of Ca^{2+}, not apparent in the case of the COO^- symmetric stretching band [20].

The band positions of COO^- stretches due to the β-COO^- group of Asp and the γ-COO^- group of Glu can be applied to the side chains of the COO^- groups of Asp and Glu of proteins, respectively: Asp $\nu_{as}(COO^-)$ 1584 cm^{-1}, $\nu_s(COO^-)$ 1402 cm^{-1} and Glu $\nu_{as}(COO^-)$ 1567 cm^{-1}, $\nu_s(COO^-)$ 1407 cm^{-1} in D_2O solution [7]. Usually, the behavior of COO^- symmetric stretch can be investigated by using protein samples in H_2O solution, where the handling of HD exchange in sample solution is not necessary. However, it is difficult to obtain information about the behavior of the COO^- antisymmetric stretch in H_2O solution, because the COO^- antisymmetric stretching band overlaps with the amide II band. Therefore, to obtain reliable infrared spectra in the region of COO^- antisymmetric stretch, exchangeable protons in the protein should be completely deuterated by incubating the apo protein dissolved in D_2O in mild heating condition (e.g. for 60 min at 60 °C). If it is difficult to exchange H for D completely for amide groups of membrane proteins and biological systems, it is suitable to analyze the COO^- symmetric stretch alone. For example, the information about the coordination structures of Ca^{2+} and Mn^{2+} has been successfully obtained for photosynthetic oxygen-evolving center [33,34].

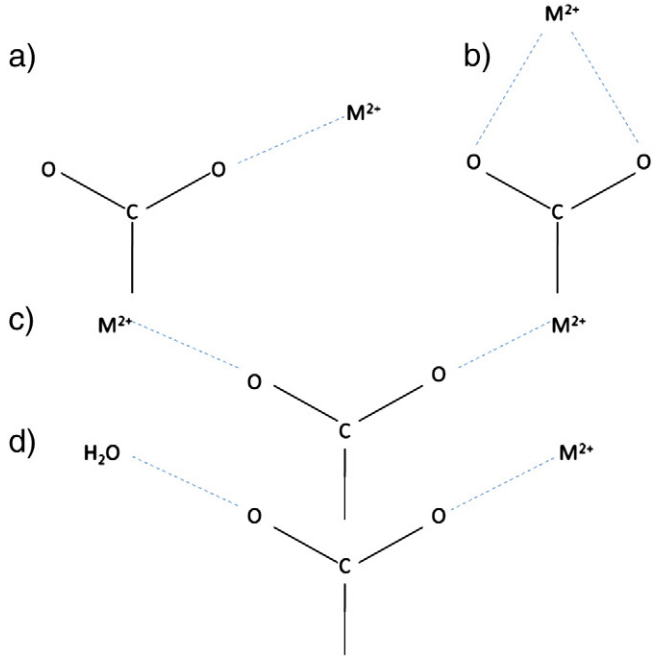

Fig. 1. Coordination structures of the side chain COO^- groups to M^{2+} in (a) unidentate, (b) bidentate, (c) bridging and (d) pseudo-bridging modes.

3. Parvalbumins

Parvalbumins (Parvs), which are ubiquitous in vertebrates, form a group in Ca^{2+}-binding proteins in parallel with calmodulin (CaM)

and troponin C (TnC) [35]. The physiological function of parvalbumins is Ca^{2+} buffer or Ca^{2+} signal modulator [36]. Parvs are classified into two distinct phylogenitic lineages, named α and β, respectively, from the comparison of amino acid sequences [37,38]. α-Parvs are in general longer by one residue and have higher pI values than β-Parvs.

Kretsinger and Nockolds [39] first reported the three-dimensional structure of carp Parv (isoform pI 4.25, β lineage) in crystal. According to their results, which Moew and Kretsinger later refined [40], this protein is globular and contains six helical parts called the A–F helices from the N-terminus, and has a feature common to Ca^{2+}-binding proteins, namely, the EF-hand motif, which is formed by about 30 amino acid residues consisting of the E and F helices (nearly perpendicular to each other) and a connecting loop with a Ca^{2+}-binding site (EF site). Another domain of about 30 amino acid residues containing the C and D helices also assumes a similar conformation to a Ca^{2+}-binding site in it (CD site). The Ca^{2+}-binding site involves a segment of a polypeptide chain having 12 continuous residues, which are arranged to coordinate to Ca^{2+} with pentagonal bipyramid symmetry, with seven ligands provided by five side-chain oxygens of the carboxylate group etc., one backbone carbonyl oxygen and one water oxygen. Two of the side chain ligands are provided by a highly conserved bidentate Glu in the 12th residue. The amino acid sequences of Ca^{2+}-binding sites for Parvs are described in Table 1, together with those of CaM and TnC.

An X-ray analysis of carp Parv pI 4.25 (β lineage) at 1.5 Å resolution by Kumar et al. [41] has shown that the Ca^{2+} ions in both the CD and EF sites are 7-coordinate; the ligands in the CD site are Asp-51, Asp-53, Ser-55 (O of the OH group), Phe-57 (O of the main chain CO group), Glu-59 and Glu-62; and those in the EF site are Asp-90, Asp-92, Asp-94, Lys-96 (O of the main-chain CO group), Glu-101 and water-128. The COO^- groups of all of these aspartic acid residues and Glu-59 bind to Ca^{2+} in the unidentate coordination mode, whereas those of Glu-62 and Glu-101 bind to Ca^{2+} in the bidentate coordination mode.

The Mg^{2+} and Mn^{2+} ions have affinities for the Ca^{2+}-binding sites in Parvs, but the association constants for Mg^{2+} are three to four orders of magnitude smaller than those for Ca^{2+} [42,43]. Pike Parv pI 4.1 is interesting for the purpose of studying the metal–ligand interactions in Ca^{2+}-binding proteins, because Declercq et al. [44,45] have reported the X-ray structures (1.6–1.8 Å resolution) of this protein for not only the Ca^{2+}-bound state but also the Mn^{2+}-bound state and a partially Mg^{2+}-bound state where the Mg^{2+} ion is bound only to the EF site. The primary structures of the two Ca^{2+}-binding sites in pike Parv pI 4.1 are exactly the same as those of carp Parv pI 4.25, and the X-ray structures of those two kinds of Parvs are essentially the same. In contrast to the Ca^{2+}-bound state, the COO^- groups of both Glu-62 and Glu-101 in the Mn^{2+}-bound state of pike Parv are unidentate. The COO^- group of Glu-101 in the partially Mg^{2+}-bound form is also unidentate.

The comparison of the FTIR spectra of the metal-bound forms (metal = Mg^{2+}, Mn^{2+} and Ca^{2+}) of pike Parv pI 4.1 leads to unique identification of bands that can be used as markers for the types of coordination of the COO^- group to the metal ion in Ca^{2+}-binding proteins. Fig. 2 shows the infrared Fourier self-deconvolved and second-derivative spectra of the Mg^{2+}-bound, Mn^{2+}-bound and Ca^{2+}-bound states of deuterated Parvs: (I) pike pI 4.1, (II) pike pI 5.0 and (III) carp pI 4.25. Significant differences are observed in the region of COO^- antisymmetric stretch; there are two bands, at 1584 and 1577 cm^{-1}, in the Mn^{2+}-bound form, while there is a single band at 1584 cm^{-1} in Fig. 2(I) a and b and at 1582 cm^{-1} in Fig. 2(I) e and f. The band at 1553 cm^{-1} in Fig. 2(I) e and f is characteristic of the Ca^{2+}-bound state.

The bands observed in the region of 1610–1550 cm^{-1} in Fig. 2(I) are correlated to the local environments of the COO^- groups in the protein molecule.

(a) The band at 1553 cm^{-1} of the Ca^{2+}-bound state is undoubtedly due to the COO^- groups of Glu-62 and Glu-101, which are coordinated to Ca^{2+} in the bidentate mode. The fact that this band is characteristic of the Ca^{2+}-bound form agrees completely to the results of X-ray analyses that the COO^- groups of Glu-62 and Glu-101 are bidentate only in the Ca^{2+}-bound form. The 1553 cm^{-1} band of the Ca^{2+}-bound form is 14 cm^{-1} downshifted from the 1567 cm^{-1} band of free glutamate. This downshift parallels that of the COO^- antisymmetric stretching band of the acetate anion ongoing from the 'ionic' state to the bidentate state.

(b) The band at 1577–1574 cm^{-1} in Fig. 2(I) c and d is probably due to the COO^- groups of Glu-62 and Glu-101 in the Mn^{2+}-bound state, which are unidentate according to X-ray analysis [45]. This band is 7–10 cm^{-1} upshifted from the 1567 cm^{-1} band of 'free' glutamate in parallel with the upshift of the acetate ion ongoing from the 'ionic' state to the unidentate. These unidentate COO^- groups may change to the pseudo-bridging coordination mode in solution, since the upshifted value of 7–10 cm^{-1} is much smaller than those observed for acetate salts going from the 'ionic' to unidentate state.

(c) According to the X-ray analysis of the partially Mg^{2+}-bound form [45], the COO^- group of Glu-101 in this form is in the pseudo-bridging state. The band at 1584 cm^{-1} of the Mg^{2+}-bound state may contain a contribution from (COO^-) of Glu-101 in the pseudo-bridging mode, in addition to the absorption due to the 'free' COO^- groups of aspartate residues.

A difference between the tertiary structure of α-Parvs and β-Parvs has been recognized after the first determination of the solution structure of a typical α-Parv (pike pI 5.0) by three-dimensional ^1H nuclear magnetic resonance spectroscopy [46]. Although the tertiary structure of pike Parv pI 5.0 retains all the features of pike Parv pI 4.1, the former differs from the latter in the length of its C-terminal F-helix domain. This domain consists of 11 residues in pike Parv pI 5.0 instead of ten in pike Parv pI 4.1. It is suggested that the lengthening of the F-helix is accompanied by the occurrence of stabilizing interactions between B and F helices. The crystal structures of two α-Parvs from leopard shark and rat have been reported [47,48]. Although shark Parv differs by nearly 50% in the amino acid sequence from pike Parv pI 4.1 and carp Parv pI 4.25, the overall structure of shark α-Parv is similar to those of the latter two typical β-Parvs. However, one important difference is that there is a locking of the tertiary

Table 1
Amino acid sequences of Ca^{2+}-binding sites for Ca^{2+}-binding proteins. Each asterisk (*) indicates the position of the amino acid residues 1, 3, 5, 7, 9 and 12, which are arranged to coordinate Ca^{2+}.

			1*	2	3*	4	5*	6	7*	8	9*	10	11	12*
Parvalbumin (Parv)	Pike pI 4.1	CD	D	Q	D	K	S	G	F	I	E	E	D	E
		EF	D	K	D	G	D	G	M	I	G	V	D	E
	Pike pI 5.0	CD	D	A	D	A	S	G	F	I	E	E	E	E
		EF	D	K	D	G	D	G	K	I	D	I	D	E
	Carp pI 4.25	CD	D	Q	D	K	S	G	F	I	E	E	D	E
		EF	D	S	D	G	D	G	K	I	D	V	D	E
Calmodulin (CaM)	Vertebrate	Site I	D	K	D	G	D	G	T	I	T	T	K	E
		Site II	D	K	D	G	N	G	T	I	D	F	P	E
		Site III	D	K	D	G	N	G	Y	I	S	A	A	E
		Site IV	D	I	D	N	D	G	Q	V	N	Y	E	E
Troponin C (TnC)	Rabbit	Site III	D	R	D	A	D	G	Y	I	D	A	E	E
	Chicken	Site III	D	K	N	A	D	G	F	I	D	I	E	E
	Akazara scallop	Site IV	D	T	D	G	S	G	T	V	D	Y	E	E

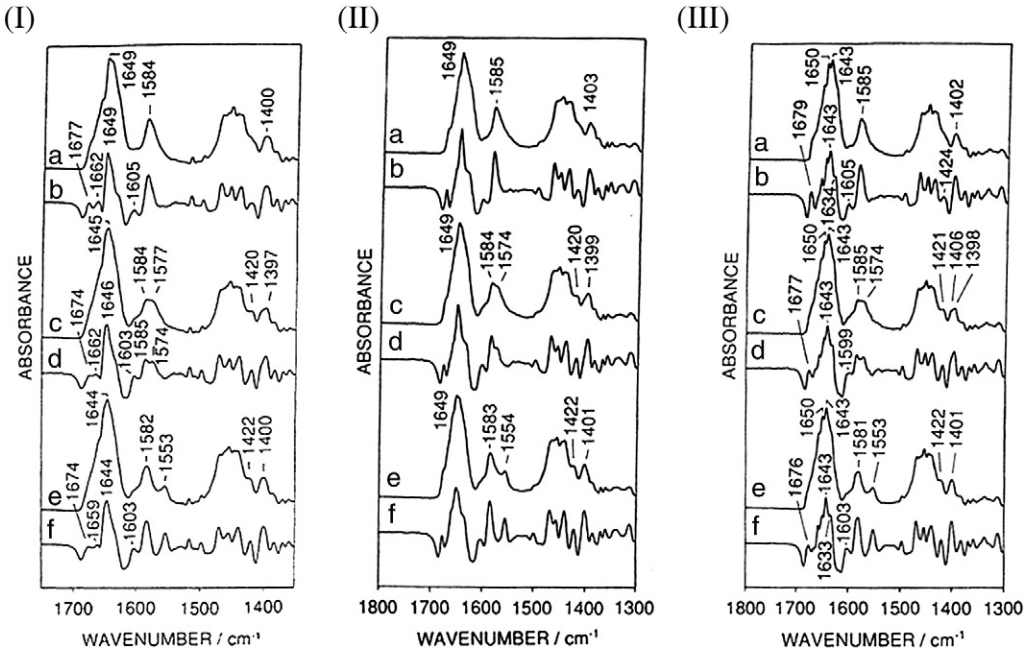

Fig. 2. Fourier self-deconvolved (a, c, e) and second-derivative (b, d, f) spectra of (a, b) Mg^{2+}-bound, (c, d) Mn^{2+}-bound, and (e, f) Ca^{2+}-bound parvalbumins: (I) pike pI 4.1, (II) pike pI 5.0 and (III) carp pI 4.25. Deconvolution was performed according to the method described by Jones and Shimokoshi [11]. Second derivatives are multiplied by −1. Fig. 2(I) is from Nara et al. [17].

structure through contacts between two sequentially distinct regions for the crystal structure of shark Parv: a hydrogen bond exists between the side-chain of Gln-108 (F-helix) and Tyr-26 (B-helix). Similarly, the crystal structure of rat α-Parv has indicated the interaction between F-helix and B-helix.

The spectral patterns of Mg^{2+}, Mn^{2+} and Ca^{2+}-bound pike Parv pI 5.0 (α lineage) (Fig. 2(II)) are, respectively, similar to those of Mg^{2+}, Mn^{2+} and Ca^{2+}-bound pike Parv pI 4.1 (β lineage) in the region of the COO^- stretching modes. The amino acid sequences for the Ca^{2+}-binding sites (CD site and EF site) are conserved between these Parvs, except for the second, fourth and 11th residues in the CD site and the second, fourth, and tenth residues in the EF site. Therefore, the similarity of the spectral patterns in the COO^- stretching modes is reasonable. The band at 1554 cm^{-1} for the Ca^{2+}-bound form is due to the COO^- groups of Glu-62 and Glu-101 binding to Ca^{2+} in the bidentate coordination mode. The band at 1574 cm^{-1} for the Mn^{2+}-bound form and the band at 1585 cm^{-1} for the Mg^{2+}-bound form are due to the COO^- groups in the pseudo-bridging coordination mode.

The most intense peaks of amide-I′ for Ca^{2+}-bound pike Parv pI 5.0 are observed at 1650 cm^{-1}, although the most intense peaks is at 1643 cm^{-1} for Ca^{2+}-bound pike Parv pI 4.1. The difference of the spectral profile in the amide I′ region between these Parvs may be due to the locking of the tertiary structure, because the secondary structure of pike Parv pI 5.0 is identical with that of pike Parv pI 4.1.

The spectral patterns of Mg^{2+}, Mn^{2+} and Ca^{2+}-bound pike Parv pI 4.25 (β lineage) (Fig. 2(III)) are, respectively, similar to those of Mg^{2+}, Mn^{2+} and Ca^{2+}-bound pike Parv pI 4.1 (β lineage) in the region of the COO^- stretching modes. The band at 1553 cm^{-1} for the Ca^{2+}-bound form reflects the side chain COO^- groups of Glu-62 and Glu-101 binding to Ca^{2+} in the bidentate coordination mode. These COO^- groups are thought to be pseudo-bridging in the Mg^{2+} and Mn^{2+}-bound forms. Therefore, the interactions of Mg^{2+}, Mn^{2+} and Ca^{2+} with ligands in carp Parv pI 4.25 are same with those in pike Parv pI 4.10.

4. Calmodulin

CaM regulates the functions of a wide variety of enzymes as a Ca^{2+} sensor [49–51]. It has four Ca^{2+}-binding sites (I–IV). X-ray analyses [52,53] have revealed that these four sites are similar to the EF-hand motif reported on parvalbumin [33], and that the COO^- groups of Asp and Glu, the $CONH_2$ group of Asn, and so on are coordinated to Ca^{2+}. Bovine CaM has 17 Asp COO^- groups and 21 Glu COO^- groups in a molecule. Of these 38 COO^- groups, 16 exist in the Ca^{2+}-binding sites, and the COO^- groups of the following 14 amino-acid residues are directly coordinated to Ca^{2+}: Asp-20 (1), Asp-22 (3), Asp-24 (5) and Glu-31(12) in site I; Asp-56 (1), Asp-58 (3) and Glu-67 (12) in site II; Asp-93 (1), Asp-95 (3) and Glu-104 (12) in site III; and Asp-129 (1), Asp-131 (3), Asp-133 (5) and Glu-140 (12) in site IV, where the numbers in parentheses refer to the local sequential order of the amino-acid residues in each Ca^{2+}-binding site consisting of 12 residues. Studies on CaM obtained from various mutants have shown that the 12th Glu residues in sites I–IV (Glu-31, Glu-67, Glu-104 and Glu-140) are essential for Ca^{2+}-binding [54], whereas the third Asp residue in site II (Asp-58) and that in site III (Asp-95) are associated with intersite cooperativity [55].

CaM binds various metal ions besides Ca^{2+} [56,57]. The correlation between CaM activities and the metal-ion radii has been studied by assaying CaM-dependent phosphodiesterase activity as well as tyrosine fluorescence [57]. FTIR and electron-spin-resonance spectroscopies and the assay of CaM-dependent myosin light-chain kinase activity have also been applied to the study of the interaction between CaM and various metal ions [58]. The interaction of CaM with Mg^{2+} is interesting because CaM is thought to interact with not only Ca^{2+} but also Mg^{2+} under physiological conditions [59]. Comparative studies on the binding effects of Ca^{2+} and Mg^{2+} have been performed by using circular dichroism [60] and nuclear magnetic resonance [61] spectroscopies and isothermal titration calorimetry [62–64]. Cd^{2+} is thought to be an effective substitute for

Ca^{2+}, since the radii of these two cations are close to each other (1.00 Å for Ca^{2+} and 0.95 Å for Cd^{2+}).

FTIR studies on CaM have been reported by Trewhella et al. [65], Rainteau et al. [58] and Jackson et al. [66], Zhang et al. [67], Nara et al. [18,19], Yuan et al. [68], Pandyra et al. [69], Jones et al. [70], Wu et al. [71], Sasakura et al. [72] and so on. The amide-I′ bands of CaM in D_2O solution have been analyzed by the method of Fourier self-deconvolution, second-derivative spectrum and difference spectrum [65]. The metal-ion dependence of the half-width of the amide-II band has been reported on undeuterated CaM in nujol [58]. The interactions of CaM with its peptides have also been studied by FTIR spectroscopy in combination with the isotope-edited method [67,68] or vibrational circular dichroism (VCD) spectroscopy [69]. The effect of the Ca^{2+} coordination structure of CaM by methionine oxidation has been investigated by FTIR [70]. Structural dynamics of CaM has been explored by using amide H–D exchange coupled with FTIR [71]. The secondary structural changes in Ca^{2+}-saturated calmodulin upon binding of an antagonist has been investigated by two-dimensional correlation analysis [72].

FTIR spectra of M^{2+}-bound CaM ($M^{2+}=Mg^{2+}$, Ca^{2+}, Sr^{2+} and Cd^{2+}) as well as M^{2+}-free (apo) CaM has been investigated in order to determine the correlations between the FTIR spectra and the function of CaM and to obtain information about structural changes induced by M^{2+} binding [16,19]. By comparing the spectra of the Ca^{2+}-bound state with those of the M^{2+}-free state, we have tried to find bands characteristic of active-type protein such as the Ca^{2+}-bound state and those of the inactive type such as the M^{2+}-free state (Fig. 3). Consequently, the marker bands of the active form are: (1) the amide-I′ band at about 1661 cm^{-1}, (2) the COO^- antisymmetric stretching band at 1553 cm^{-1} and (3) the COO^- symmetric stretching band at 1424 cm^{-1}.

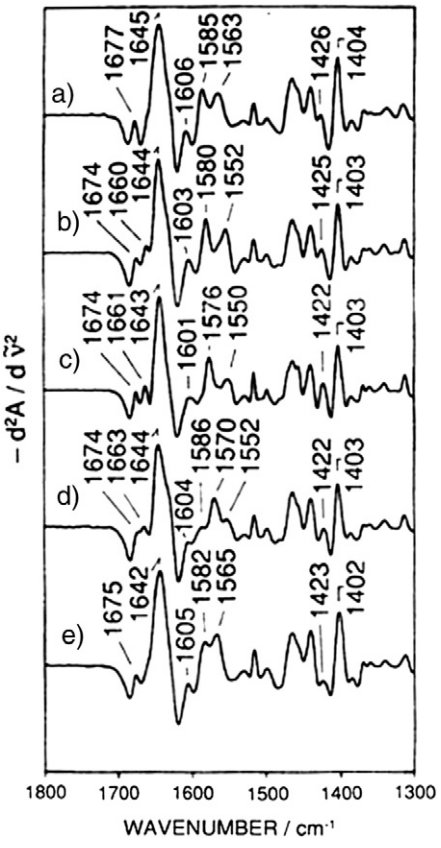

Fig. 3. FTIR second-derivative spectra of the M^{2+}-bound and M^{2+}-free (apo) states of calmodulin in D_2O solution: (a) Mg^{2+}-bound state; (b) Ca^{2+}-bound state; (c) Sr^{2+}-bound state; (d) Cd^{2+}-bound state; and (e) M^{2+}-free state.
From Nara et al. [19].

5. Akazara scallop troponin C

Muscle contraction of vertebrate skeletal and cardiac muscles is regulated by troponin in a Ca^{2+}-dependent manner [73]. Troponin contains three components: TnC, troponin I and troponin T. TnC is the Ca^{2+}-binding component. In general, TnC contains two independent Ca^{2+}-binding domains, each consisting of two EF-hand motifs [74]. Vertebrate TnCs bind three or four Ca^{2+} ions in a molecule [75–77] and act as the Ca^{2+} switch of muscle contraction associated with the binding and release of one or two Ca^{2+} ions in the N-terminal domain. The N-terminal domain has thus been called the regulatory domain and contains one or two low-affinity Ca^{2+}-binding sites [78]. On the other hand, the C-terminal domain has been called the structural domain and contains two high-affinity sites. They also bind Mg^{2+} and are called Ca^{2+}/Mg^{2+} sites. Although the N-terminal low-affinity sites are called Ca^{2+}-specific sites, they also bind Mg^{2+} very weakly [79,80]. Since the intracellular Mg^{2+} concentration is relatively high at about 1 mM [81,82], intracellular Mg^{2+} ions are bound to the low-affinity Ca^{2+}-binding sites in addition to high-affinity sites in resting muscle cells [80]. It is therefore important to know the structural differences between the Ca^{2+}- and Mg^{2+}-bound forms.

Invertebrate muscles also have troponin molecules, and their TnCs bind less Ca^{2+} than do vertebrate ones, because they have lost the Ca^{2+}-binding ability at several sites due to the replacement of amino acids critical to chelate Ca^{2+} [83]. Akazara scallop is an invertebrate. Its striated adductor muscle contains TnC that works as a Ca^{2+} switch of contraction [84], and it binds only one Ca^{2+} ion at the C-terminal EF-hand motif [85]. Akazara scallop TnC is thus a curious and interesting molecule, since it regulates muscle contraction by binding a single Ca^{2+} ion.

The Ca^{2+}-binding loop (site IV) of this protein is composed of DTDGSGTVDYEE (residues 131–142) [85]. Applying the general rule of the EF-hand motif [41,42] to this protein, the COO^- groups of Asp-131, Asp-133 and Glu-142 should coordinate to Ca^{2+} directly. On the basis of the crystal structure of vertebrate TnCs [86,87] and C-terminal domain of Akazara scallop TnC in complex with a troponin I fragment [88,89], the COO^- group of Glu at the 12th position in site IV may coordinate to the Ca^{2+} ion in the bidentate mode and to the COO^- groups of Asp at the 1st and 3rd positions in the unidentate mode.

Fig. 4 shows the FTIR absorbance and second-derivative spectra of apo, Mg^{2+}-bound and Ca^{2+}-bound Akazara scallop TnC in D_2O across the range of 1750–1350 cm^{-1}. Fig. 5 shows the 1750–1350 cm^{-1} region of the difference spectra between the M^{2+}-bound and apo states. The bands in the COO^- antisymmetric stretching region for Akazara scallop TnC have been interpreted in relation to the coordination structures of the COO^- group and the peak positions of COO^- stretching bands mentioned above. 1) The 1543–cm^{-1} band in Fig. 4c is due to side-chain Glu-142 COO^- coordinated to the Ca^{2+} ion in the bidentate mode. This band is not observed in the Mg^{2+}-bound state, and the intensity at 1567 cm^{-1} in the Mg^{2+}-bound state is the same as that in the apo state. Therefore, this COO^- group is not coordinated to Mg^{2+} directly. 2) The bands at 1602 cm^{-1} for the Mg^{2+}-bound state in Fig. 5a and at 1592 cm^{-1} for the Ca^{2+}-bound state in Fig. 5b indicate that the COO^- groups of Asp-131 and Asp-133 interact with Ca^{2+} and Mg^{2+} in the pseudo-bridging mode. This is direct evidence that Akazara scallop TnC interacts with Mg^{2+} in the single Ca^{2+}-binding site. 3) The shift of the COO^- symmetric stretch from 1396 to 1425 cm^{-1} in Fig. 5a also reflects that the COO^- groups interact with Mg^{2+} in the pseudo-bridging mode, because the peak positions for the COO^- symmetric and antisymmetric stretching vibrations move together. In addition, the weak band at 1605 cm^{-1} for the apo state and at 1610 cm^{-1} for the Ca^{2+}-bound state may be due to side-chain COO^- groups.

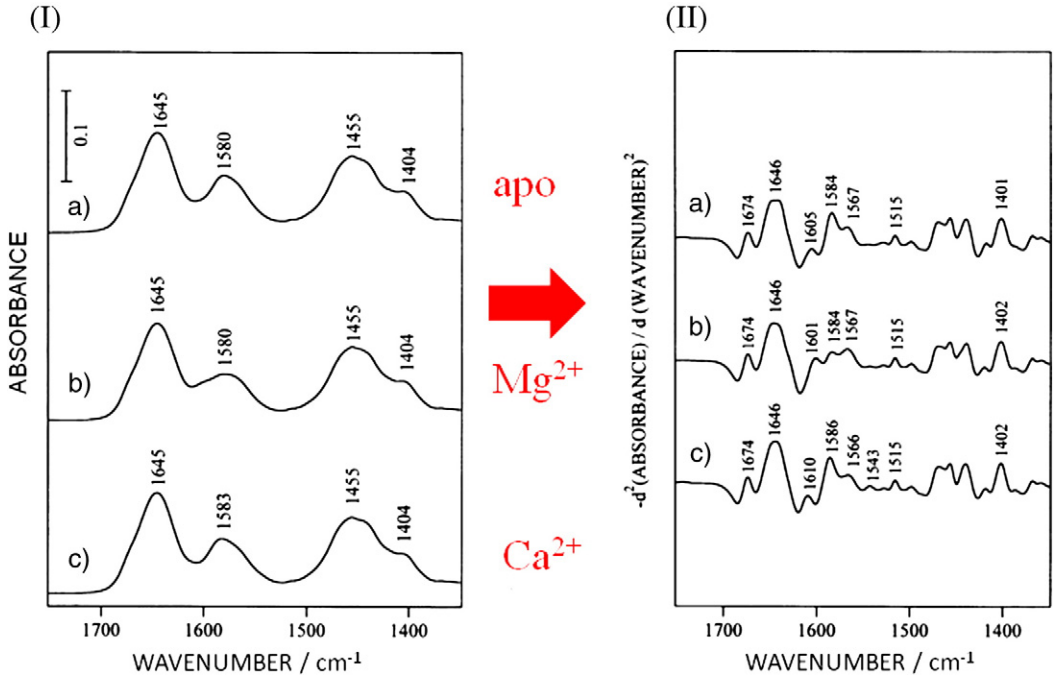

Fig. 4. (I) FTIR absorbance spectra and (II) FTIR second-derivative spectra of (a) M^{2+}-free, (b) Mg^{2+}-bound and (c) Ca^{2+}-bound Akazara scallop troponin C in solutions containing 40 mM HEPES-NaOD (pD 7.4) and 100 mM KCl.
From Yumoto et al. [23].

As a result, a model for the on–off mechanism in the activation of Akazara scallop TnC has been proposed (Fig. 6). The Mg^{2+}-bound and Ca^{2+}-bound states may be regarded, respectively, as the resting and activated ones for muscle contraction, although the apo state may be the resting one under physiological conditions. First, in the Mg^{2+}-bound state, Asp-131 and Asp-133 interact with the Mg^{2+} ion in the pseudo-bridging mode, whereas Glu-142 does not interact with the Mg^{2+} ion. Asp-139 may be a ligand for the Mg^{2+} ion. Next, when Mg^{2+} is replaced by Ca^{2+} in the binding site by the stimulation, Glu-142 interacts with the Ca^{2+} ion in the bidentate mode, whereas Asp-131 and Asp-133 interact with the Ca^{2+} ion in the pseudo-bridging mode. The Ca^{2+} affinity is higher than the Mg^{2+} affinity, because Mg^{2+} has been easily replaced by Ca^{2+} but Ca^{2+} has not been easily replaced by Mg^{2+} [23]. The Glu-142 COO^- group plays a critical role in the selectivity between Ca^{2+} and Mg^{2+} for the Ca^{2+}-binding site and may be critical for the affinity for Ca^{2+}. Thus, it has been recognized that the side-chain COO^- groups in the Ca^{2+}-binding site are important for the interaction of EF-hand proteins with divalent metal ions and the selectivity between Mg^{2+} and Ca^{2+}. The result about the Mg^{2+} ligation by Akazara scallop TnC is close to the model proposed by Malmendal et al. [90]; Mg^{2+} binding occurs without ligation of the side-chain COO^- of Glu at the 12th position in the Ca^{2+}-binding loops of CaM.

FTIR spectroscopy has also been applied to study the coordination structure of a divalent cation (M^{2+} = Mg^{2+}, Ca^{2+}, Sr^{2+} and Ba^{2+}) bound in the E142D mutant (the mutant protein where Glu-142 residue is replaced with Asp) and the wild-type TnC C-terminal lobe (C-lobe) [88,91]. The results have shown that the side chain COO^- group of Asp142 does not directly bind to Sr^{2+} or Ba^{2+}, although the side chain COO^- group of Glu at the 12th position of the

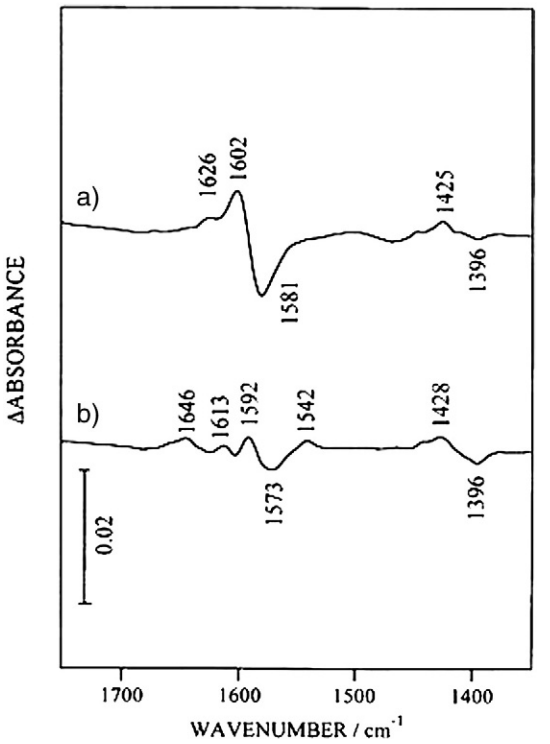

Fig. 5. FTIR difference spectra of Akazara scallop troponin C induced by (a) Mg^{2+} binding and (b) Ca^{2+} binding.
From Yumoto et al. [23].

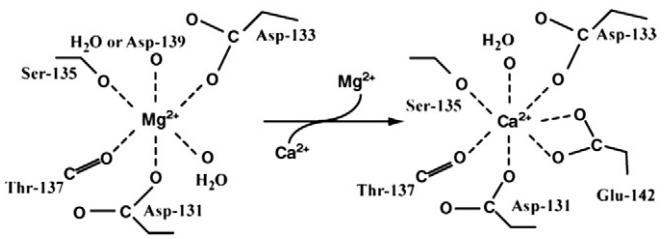

Fig. 6. A schematic model of changes in coordination structure of the Ca^{2+}-binding site of Akazara scallop troponin C accompanying the exchange of Mg^{2+} with Ca^{2+}.
From Yumoto et al. [23].

wild-type TnC C-lobe binds to these ions in the bidentate coordination mode [27]. This result suggests that the shortage of a methylene group is critical for the M^{2+} coordination structure of Akazara scallop TnC.

The spectral pattern of the Ba^{2+}-loaded state is almost identical with that of the M^{2+}-free state, and it therefore is not clear whether E142D binds to Sr^{2+} or Ba^{2+}. We have confirmed whether the E142D mutant binds to them by adding Sr^{2+} or Ba^{2+} to the Mg^{2+}-loaded form because Mg^{2+}-loaded E142D mutant shows a characteristic band at 1600 cm^{-1}, which is due to the Asp side chain COO^- groups binding to Mg^{2+} in the pseudo-bridging coordination mode [27]. As a result, Mg^{2+} is completely replaced by Sr^{2+} but partially replaced by Ba^{2+} in site IV, suggesting that the affinity of the E142D mutant for Ba^{2+} is weaker than that for Sr^{2+}. Based on the Mg^{2+}–M^{2+} exchange experiments, the affinity of E142D mutant for M^{2+} is in the order: $Ca^{2+} \sim Sr^{2+} > Mg^{2+} \sim Ba^{2+}$ [27].

The absence of a methylene group of Glu at the 12th position is critical for Ca^{2+} binding because the side chain COO^- group of Asp142 for the E142D mutant does not bind to Ca^{2+} (ion radius, 1.00 Å) in the bidentate coordination mode. By using the wild-type TnC C-lobe, it is confirmed that the side chain COO^- group of Glu at the 12th position in site IV binds to Ca^{2+}, Sr^{2+}, and Ba^{2+} in the bidentate coordination. The absence of a methylene group is not compensated for by a larger metal ion such as Sr^{2+} (ion radius, 1.13 Å) or Ba^{2+} (ion radius, 1.33 Å). The interaction of the Asp142 side chain COO^- group with Sr^{2+} or Ba^{2+} is not observed, suggesting that Asp142 may not directly participate in Sr^{2+} or Ba^{2+} binding.

6. Synthetic peptide analogues of Ca^{2+}-binding site

The use of the synthetic calcium-binding peptide approach has provided valuable results for understanding the calcium-binding properties thus far [92–95]. Calcium binding to a series of peptides derived from site III of rabbit skeletal muscle TnC has been studied by Reid et al. [92], who found that a 34-residue peptide is required for relatively tight calcium binding. Shorter peptides have decreased calcium affinity, and the isolated 12-residue Ca^{2+}-binding loop binds to Ca^{2+} very weakly [93]. Thus, the length of the peptide is important for Ca^{2+} binding.

The coordination structures of Ca^{2+} ion bound to synthetic peptide analogues of the calcium-binding site III of rabbit skeletal muscle TnC have been investigated by FTIR spectroscopy [16,26]. The 34-residue peptide corresponding to the EF hand motif (helix–loop–helix) has showed a band at 1552 cm^{-1} in the Ca^{2+}-loaded state, indicating that the side chain COO^- group of Glu at the 12th position serves as a ligand for Ca^{2+} in the bidentate coordination mode [26]. The 13-residue peptide (Ac-DRDADGYIDAEEL-NH_2) containing the Ca^{2+}-binding site III (DRDADGYIDAEE) does not show such spectral patterns in the Ca^{2+}-loaded state, meaning that shorter synthetic peptide corresponding to site III has less or no affinity for Ca^{2+} [26]. The 17-residue peptide (Ac-DRDADGYIDAEELAEIF-NH_2) is the minimum peptide necessary for the interaction of side-chain COO^- of Glu at the 12th position with Ca^{2+} in the bidentate coordination mode [26].

FTIR second-derivative spectra have been investigated for synthetic 17-residue peptide analogues for Site IV of Akazara scallop TnC (wild type) [Ac-DTDGSGTVDYEEFKBLM-NH_2] and for site-directed mutated ones (E142D, E142Q and E142A) in the apo- and Ca^{2+}-loaded states (Fig. 7) [16,25]. The peptide analogue for the wild type shows a band at 1545 cm^{-1} in the Ca^{2+}-loaded state, which is not observed in the apo state. This band is almost the same as that at 1543 cm^{-1} for Ca^{2+}-bound wild-type Akazara scallop TnC. Therefore, the band at 1543 cm^{-1} is undoubtedly assigned to the Glu-142 side-chain COO^- binding to Ca^{2+} in the bidentate coordination mode. The peptide analogues for site-directed mutants such as E142D, E142Q and E142A showed

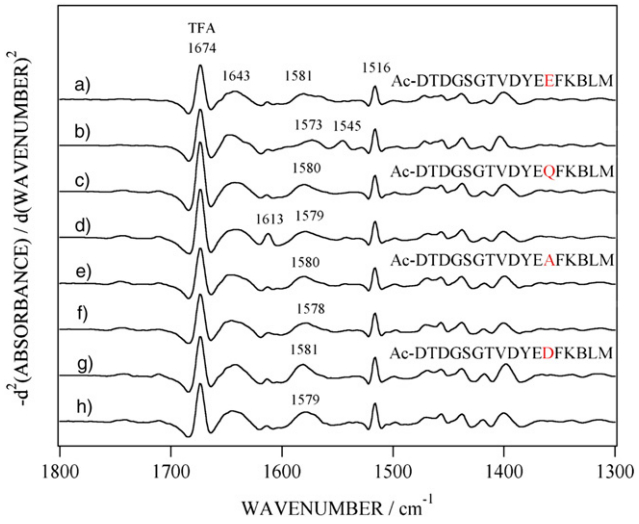

Fig. 7. Infrared second-derivative spectra for synthetic 17-residue peptide analogues for site IV of Akazara scallop TnC (wild type) in (a) the apo- and (b) the Ca^{2+}-loaded states, E142D mutant in (c) the apo- and (d) the Ca^{2+}-loaded states, E142Q mutant in (e) the apo- and (f) the Ca^{2+}-loaded states and E142A mutant in (g) the apo- and (h) the Ca^{2+}-loaded states in D_2O solution. The amino acid sequences are Ac-DTDGSGTVDYEEFKBLM-NH_2 for the wild type, Ac-DTDGSGTVDYEDFKBLM-NH_2 for the E142D mutant, Ac-DTDGSGTVDYEQFKBLM-NH_2 for the E142Q mutant and Ac-DTDGSGTVDYEAFKBLM-NH_2 for the E142A mutant. The band at 1674 cm^{-1} is mainly due to trifluoroacetate (TFA), which is thought to be introduced during purification.
From Nara et al. [25].

no band around 1545 cm^{-1} even in the Ca^{2+}-loaded state (Fig. 7). These results are consistent with those of the E142D and E142Q mutants of Akazara scallop TnC. Consequently, it has been confirmed that the assignment of 1543 cm^{-1} for Ca^{2+}-bound Akazara scallop TnC described above using the synthetic peptide analogue approach is correct.

The physiological activity of Akazara scallop TnC has been reported only in the wild-type and E142Q forms [96]. The Ca^{2+}-loaded E142Q mutant is inactive due to the replacement of E with Q at the 12th position of site IV. The E142D mutant also may be inactive in the Ca^{2+}-loaded state, because the side-chain COO^- group at the 12th position does not serve as the ligand for Ca^{2+} directly. To elucidate the function of Akazara scallop TnC, it will be necessary to investigate not only TnC alone but also the troponin complex.

We summarize the COO^- antisymmetric stretching band positions of COO^- groups of Glu in the bidentate coordination mode at the 12th position of the calcium binding sites for various EF-hand

Table 2
The COO^- antisymmetric stretching band positions of COO^- groups of Glu in the bidentate coordination mode at the 12th position of the calcium binding sites for various EF-hand Ca^{2+}-binding proteins and model peptide analogues.

Proteins or peptides	$\nu_{asym}(COO^-)$	Reference
Parvalbumin pike pI 4.1	1553 cm^{-1}	Fig. 2(I), Nara et al. [17]
Parvalbumin pike pI 5.0	1554 cm^{-1}	Fig. 2(II)
Parvalbumin carp pI 4.25	1553 cm^{-1}	Fig. 2(III)
Bovine calmodulin	1552 cm^{-1}	Fig. 3, Nara et al. [18,19]
Rabbit skeletal muscle troponin C site III	1552 cm^{-1}	Nara et al. [26]
Akazara scallop troponin C wild type	1543 cm^{-1}	Fig. 4, Yumoto et al. [23]
E142Q mutant, E142D mutant	x	Nara et al. [16,25,26]
recoverin	1544 cm^{-1}	Ozawa et al. [22]
Ac-DRDADGYIDAEELAEIF-NH_2	1555 cm^{-1}	Nara et al. [26]
Ac-DTDGSGTVDYEEFKBLM-NH_2	1545 cm^{-1}	Nara et al. [25]
EF-hand proteins in the apo state	x	Nara et al. [16]
α-lactalbumin, equine lysozyme (non EF)	x	Mizuguchi et al. [20,21]

Ca^{2+}-binding proteins and model peptide analogues in Table 2. First, FTIR for non EF hand Ca^{2+}-binding proteins such as α-lactalbumin [20], equine lysozyme [21] and so on, do not show the band due to the bidentate COO^- groups over the range of 1555 to 1540 cm^{-1}, because these proteins do not contain the COO^- groups binding to Ca^{2+} in the bidentate coordination mode. Needless to say, FTIR spectra for EF-hand proteins in the apo state do not show this band. As for the COO^- groups of Glu at the 12th position binding to Ca^{2+} in the bidentate coordination mode, representative EF-hand proteins such as parvalbumins, CaM and vertebrate TnC show a band at 1555–1550 cm^{-1} in the Ca^{2+}-bound state, while Akazara scallop TnC and recoverin [22] show the corresponding band at 1545–1542 cm^{-1} in the Ca^{2+}-bound state. These differences are thought to reflect the structural difference of the COO^- groups, as expected from the *ab initio* molecular orbital calculation [31]. Interestingly, the band positions for the site III of rabbit skeletal muscle TnC (1552 cm^{-1}) and Akazara scallop (1543 cm^{-1}) are, respectively, consistent with those of corresponding synthetic Ca^{2+}-binding peptide analogues (1553 cm^{-1} [16,26] and 1545 cm^{-1} [16,25]), which are composed of 17 residues, within 4 cm^{-1} error. Therefore, the Ca^{2+} coordination structure of these proteins are conserved for the 17-residue synthetic peptide analogues and therefore 17-residue synthetic peptide analogues are expected to become good model compounds for understanding the coordination structures of Ca^{2+}.

7. Concluding remarks

FTIR spectroscopy is a powerful tool for identifying the coordination structures of M^{2+} in Ca^{2+}-binding proteins—that is, the coordination structure modes of side-chain COO^- groups. The downshift of the COO^- antisymmetric stretching mode from 1565 cm^{-1} to 1555–1540 cm^{-1} upon Ca^{2+} binding is a commonly observed feature of FTIR spectra for EF-hand proteins. As can be seen from FTIR difference spectra of Akazara scallop TnC induced by Mg^{2+} binding and Ca^{2+} binding (Fig. 5), the upshift of the symmetric stretching does not only mean that the COO^- group binds to M^{2+} in the bidentate coordination mode, but that the COO^- group binds to M^{2+} in the pseudo-bridging coordination mode. Therefore, it is suitable to analyze the region of COO^- antisymmetric stretch in D_2O solution in order to determine the coordination mode of COO^- groups of EF-hand proteins correctly. Investigating synthetic peptide analogues by FTIR spectroscopy in combination with site-directed mutagenesis, will make it possible to more clearly identify the specific amino acid residues involved in the coordination of metals to Ca^{2+}-binding proteins.

References

[1] H.H. Mantsch, H.L. Casel, D.M. Moffat, in: R.J.H. Clark, R.E. Hester (Eds.), Spectroscopy of Biological Systems, Wiley, Chichester, 1986, pp. 1–46.
[2] J.L.R. Arrondo, A. Muga, J. Castresana, F.M. Goñi, Quantitative studies of the structure of proteins in solution by Fourier-transform infrared spectroscopy, Prog. Biophys. Mol. Biol. 59 (1991) 23–56.
[3] D.M. Byler, H. Susi, Examination of the secondary structure of proteins by deconvolved FTIR spectra, Biopolymers 25 (1986) 469–487.
[4] W.K. Surewicz, H.H. Mantsch, New insight into protein secondary structure from resolution-enhanced infrared-spectra, Biochim. Biophys. Acta 952 (1988) 115–130.
[5] M. Jackson, P.I. Haris, D. Chapman, Fourier-transform infrared spectroscopic studies of lipids, polypeptides and proteins, J. Mol. Struct. 214 (1989) 329–355.
[6] W.K. Surewicz, H.H. Mantsch, D. Chapman, Determination of protein secondary structure by Fourier-transform infrared-spectroscopy. A critical assessment, Biochemistry 32 (1993) 389–394.
[7] A. Barth, The infrared absorption of amino acid side chains, Prog. Biophys. Mol. Biol. 74 (2000) 141–173.
[8] A. Barth, C. Zscherp, What vibrations tell us about proteins, Q. Rev. Biophys. 35 (2002) 369–430.
[9] J.K. Kauppinen, D.J. Moffatt, H.H. Mantsch, D.G. Cameron, Fourier self-deconvolution—a method for resolving intrinsically overlapped bands, Appl. Spectrosc. 35 (1981) 271–276.
[10] J.K. Kauppinen, D.J. Moffatt, H.H. Mantsch, D.G. Cameron, Fourier-transforms in the computation of self-deconvoluted and 1st-order derivative spectra of overlapped band contours, Anal. Chem. 53 (1981) 1454–1457.
[11] R.N. Jones, K. Shimokoshi, Some observations of the resolution enhancement of spectral data by the method of self-deconvolution, Appl. Spectrosc. 37 (1983) 59–67.
[12] I. Noda, Advances in two-dimensional correlation spectroscopy, Vib. Spectrosc. 36 (2004) 143–165.
[13] I. Noda, Recent advancement in the field of two-dimensional correlation spectroscopy, J. Mol. Struct. 883 (2008) 2–26.
[14] Y. Ozaki, K. Murayama, Y. Wu, B. C-Matusewicz, Two dimensional infrared correlation spectroscopy studies on secondary structures and hydrogen bondings of side chains of proteins, Spectrosc. Int. J. 17 (2003) 79–100.
[15] W.W. Wright, J.M. Vanderkooi, Use of IR absorption of the carboxyl group of amino acids, and their metabolites to determine pKs, to study proteins, and to monitor enzymatic activity, Biospectroscopy 3 (1997) 457–467.
[16] M. Nara, M. Tanokura, Infrared spectroscopic study of the metal-coordinations structures of calcium-binding proteins, Biochem. Biophys. Res. Commun. 369 (2008) 225–239.
[17] M. Nara, M. Tasumi, M. Tanokura, T. Hiraoki, M. Yazawa, A. Tsutsumi, Infrared studies of interaction between metal ions and Ca^{2+}-binding proteins. Marker bands for identifying the types of coordination of the side-chain COO^- groups to metal ions in pike parvalbumin (pI = 4.10), FEBS Lett. 349 (1994) 84–88.
[18] M. Nara, M. Tanokura, M. Tasumi, UV-laser induced changes in the infrared spectrum of calmodulin in the presence of a photosensitive Ca^{2+} chelator, J. Mol. Struct. 324 (1994) 107–112.
[19] M. Nara, M. Tanokura, T. Yamamoto, M. Tasumi, A comparative study of the binding effects of Mg^{2+}, Ca^{2+}, Sr^{2+}, and Cd^{2+} on calmodulin by Fourier-transform infrared spectroscopy, Biospectroscopy 1 (1995) 47–54.
[20] M. Mizuguchi, M. Nara, K. Kawano, K. Nitta, FTIR study of the Ca^{2+}-binding to bovine α-lactalbumin. Relationships between the type of coordination and characteristics of the bands due to the Asp COO^- groups in the Ca^{2+}-binding site, FEBS Lett. 417 (1997) 153–157.
[21] M. Mizuguchi, M. Nara, Y. Ke, K. Kawano, T. Hiraoki, K. Nitta, Fourier-transform infrared spectroscopic studies on the coordination of the side-chain COO^- groups to Ca^{2+} in equine lysozyme, Eur. J. Biochem. 250 (1997) 72–76.
[22] T. Ozawa, M. Fukuda, M. Nara, A. Nakamura, Y. Komine, K. Kohama, Y. Umezawa, How can Ca^{2+} selectively activate recoverin in the presence of Mg^{2+}? Surface plasmon resonance and FT-IR spectroscopic studies, Biochemistry 39 (2000) 14495–14503.
[23] F. Yumoto, M. Nara, H. Kagi, W. Iwasaki, T. Ojima, K. Nishita, K. Nagata, M. Tanokura, Coordination structures of Ca^{2+} and Mg^{2+} in Akazara scallop troponin C in solution. FTIR spectroscopy of side-chain COO^- groups, Eur. J. Biochem. 268 (2001) 6284–6290.
[24] M. Nara, F. Yomoto, K. Nagata, M. Tanokura, H. Kagi, T. Ojima, K. Nishita, Fourier transform infrared spectroscopic study on the binding of Mg^{2+} to a mutant Akazara scallop troponin C (E142Q), Biopolymers 268 (2004) 77–81.
[25] M. Nara, F. Yomoto, K. Nagata, M. Tanokura, H. Kagi, T. Ojima, K. Nishita, Infrared spectroscopic study on Ca^{2+} binding to Akazara scallop troponin C in comparison with peptide analogues of its Ca^{2+}-binding site IV, Vib. Spectrosc. 42 (2006) 188–191.
[26] M. Nara, H. Morii, F. Yumoto, H. Kagi, M. Tanokura, Fourier transform infrared spectroscopic study on the Ca^{2+}-bound coordination structures of synthetic peptide analogues of the calcium-binding site III of troponin C, Biopolymers 82 (2006) 339–343.
[27] M. Nara, F. Yumoto, H. Kagi, M. Tanokura, Infrared spectroscopic study of the binding of divalent cations to Akazara scallop troponin C: the effect of the methylene side chain of glutamate residues, Biopolymers 89 (2008) 595–599.
[28] G.B. Deacon, R.J. Phillips, Relationships between the carbon–oxygen stretching frequencies of carboxylato complexes and the type of carboxylate coordination, Coord. Chem. Rev. 33 (1980) 227–250.
[29] K. Nakamoto, in: Infrared and Raman Spectra of Inorganic and Coordination Compounds Part B, 5th edn, Wiley, New York, 1997, pp. 57–62.
[30] J.E. Tackett, FT-IR characterization of metal acetates in aqueous-solution, Appl. Spectrosc. 43 (1989) 483–499.
[31] M. Nara, H. Torii, M. Tasumi, Correlation between the vibrational frequencies of the carboxylate group and the types of its coordination to a metal ion: an *ab initio* molecular orbital study, J. Phys. Chem. 100 (1996) 19812–19817.
[32] T. Dudev, C. Lim, The effect of metal binding on the characteristic infrared band intensities of ligands of biological interest, J. Mol. Struct. 1009 (2012) 83–88.
[33] T. Noguchi, T. Ono, Y. Inoue, Direct detection of a carboxylate bridge between Mn and Ca^{2+} in the photosynthetic oxygen-evolving center by means of Fourier transform infrared spectroscopy, Biochim. Biophys. Acta 1228 (1995) 189–200.
[34] M. Iizawa, H. Suzuki, T. Nogichi, Orientation of carboxylate groups coupled to the Mn cluster in the photosynthetic oxygen-evolving center as studied by polarized ATR-FTIR spectroscopy, Biochemistry 49 (2010) 3074–3082.
[35] J.F. Pechère, in: R.H. Wasserman, R. Corradino, E. Carafoli, R.H. Kretsinger, D.H. MacLennan, F.L. Siegel (Eds.), Calcium-binding Protein and Calcium, Elsevier, New York, 1977, pp. 213–221.
[36] B. Schwaller, The use of transgenic mouse models to reveal the functions of Ca^{2+} buffer proteins in excitable cells, Biochim. Biophys. Acta 1820 (2012) 1294–1303.
[37] M. Goodman, J.F. Pechère, Evolution of muscular parvalbumins investigated by maximum parsimony method, J. Mol. Evol. 9 (1977) 131–158.
[38] M. Goodman, J.F. Pechère, J. Haiech, J.G. Demaille, Evolutionary diversification of structure and function in the family of intracellular calcium-binding proteins, J. Mol. Evol. 13 (1977) 331–352.

[39] R.H. Kretsinger, C.E. Nockolds, Ionic interactions with parvalbumins. Crystal structure determination of pike 4.10 parvalbumin in four different ionic environments, J. Biol. Chem. 248 (1973) 3313–3326.
[40] P.C. Moews, R.H. Kretsinger, Refinement structure of carp muscle calcium-binding parvalbumin by model-building and difference Fourier-analysis, J. Mol. Biol. 91 (1975) 201–225.
[41] V.D. Kumar, L. Lee, B.F.P. Edwards, Refined crystal-structure of calcium-liganded carp parvalbumin 4.25 at 1.5-Å resolution, Biochemistry 29 (1990) 1404–1412.
[42] P. Lehky, M. Comte, E.H. Fischer, E.A. Stein, New solid-phase chelator with high affinity and selectivity for calcium—parvalbumin-polyacrylamide, Anal. Biochem. 82 (1977) 158–169.
[43] W. Wunk, J.A. Cox, E.A. Stein, in: W.Y. Cheung (Ed.), Calcium and Cell Function, vol. 2, Academic Press, New York, 1982, pp. 243–278.
[44] J.P. Declercq, B. Tinant, J. Parello, G. Etienne, R. Huber, Crystal-structure determination and refinement of pike 4.10 parvalbumin (minor component *Esox lucius*), J. Mol. Biol. 202 (1988) 349–353.
[45] J.-P. Declercq, B. Tinant, J. Parello, J. Rambaud, Ionic interactions with parvalbumins. Crystal structure determination of pike 4.10 parvalbumin in four different ionic environments, J. Mol. Biol. 220 (1991) 1017–1039.
[46] A. Padilla, G.W. Vuister, R. Boelens, G.J. Kleywegt, A. Cavé, J. Parello, R. Kaptein, Homonuclear 3-dimensinal H-1-NMR spectroscopy of pike parvalbumin-comparison of short-range and medium-range NOEs from 2D and 3D NMR, J. Am. Chem. Soc. 112 (1990) 5024–5030.
[47] F. Roquet, J.-P. Declercq, B. Tinant, J. Rambaud, J. Parello, Crystal-structure of the unique parvalbumin component from muscle of the leopard shark (*Triakis semifasciata*) — the 1st X-ray study of an α-parvalbumin, J. Mol. Biol. 223 (1992) 705–732.
[48] C.A. McPhalen, A.R. Sielecki, B.D. Santarsiero, M.N.G. James, Refined crystal-structure of rat parvalbumin, a mammalian α-lineage parvalbumin, at 2.0-Å resolution, J. Mol. Biol. 235 (1994) 718–732.
[49] C.B. Klee, T.H. Crouch, P.G. Richman, Calmodulin, Annu. Rev. Biochem. 49 (1980) 489–515.
[50] C.B. Klee, T.C. Vanaman, Calmodulin, Adv. Protein Chem. 35 (1982) 213–321.
[51] J.A. Cox, Interactive properties of calmodulin, Biochem. J. 249 (1988) 621–629.
[52] Y.S. Babu, J.S. Sack, T.J. Greenhough, C.E. Bugg, A.R. Means, W.J. Cook, Three-dimensional structure of calmodulin, Nature 315 (1985) 37–40.
[53] Y.S. Babu, C.E. Bugg, W.J. Cook, Structure of calmodulin refined at 2.2 Å resolution, J. Mol. Biol. 204 (1988) 191–204.
[54] J.F. Maune, C.B. Klee, K. Beckingham, Ca^{2+}-binding and conformational change in two series of point mutations to the individual Ca^{2+}-binding sites of calmodulin, J. Biol. Chem. 267 (1992) 5286–5295.
[55] Y. Waltersson, S. Linse, P. Brodin, T. Grundstrom, Mutational effects on the cooperativity of Ca^{2+}-binding in calmodulin, Biochemistry 32 (1993) 7866–7871.
[56] D.J. Wolff, P.G. Poireir, C.O. Brostrom, M.A. Brostrom, Divalent cation binding properties of bovine brain Ca^{2+}-dependent regulator protein, J. Biol. Chem. 252 (1977) 4108–4117.
[57] S. Chao, Y. Suzuki, J.R. Zysk, W.Y. Cheung, Activation of calmodulin by various metal cation as a function of ionic radius, Mol. Pharmacol. 26 (1984) 75–82.
[58] D. Rainteau, C. Wolf, F. Lavialle, Effects of calcium and calcium analogues of calmodulin: a Fourier transform infrared and electron spin resonance investigation, Biochim. Biophys. Acta. 1011 (1989) 81–87.
[59] J. Haiech, C.B. Klee, abd G. Demaille, Effects of cations on affinity of calmodulin for calcium: ordered binding of calcium ions allows the specific activation of calmodulin-stimulated enzymes, Biochemistry 20 (1981) 3890–3897.
[60] J.R. Dedman, J.D. Potter, R.L. Jackson, J.D. Johnson, A.R. Means, Physicochemical properties of rat testis Ca^{2+}-dependent regulator protein of cyclic nucleotide phosphodiesterase, J. Biol. Chem. 25 (1977) 8415–8422.
[61] K.B. Seamon, Calcium and magnesium-dependent conformational states of calmodulin as determined by nuclear magnetic resonance, Biochemistry 19 (1980) 207–215.
[62] M. Tanokura, K. Yamada, Heat capacity and entropy changes of calmodulin induced by calcium binding, J. Biochem. 95 (1984) 643–649.
[63] M. Tanokura, K. Yamada, Effects of trifluoperazine on calcium binding by calmodulin. Heat capacity and entropy changes, J. Biol. Chem. 261 (1986) 10749–10752.
[64] M. Tanokura, K. Yamada, A calorimetric study of Ca^{2+} binding by wheat germ calmodulin. Regulatory steps driven by entropy, J. Biol. Chem. 268 (1993) 7090–7092.
[65] J. Trewhella, W.K. Liddle, D.B. Heidorn, N. Strynadka, Calmodulin and troponin C structures studied by Fourier transform infrared spectroscopy: effects of Ca^{2+} and Mg^{2+} binding, Biochemistry 28 (1989) 1294–1301.
[66] M. Jackson, P.I. Haris, D. Chapman, Fourier-transform infrared spectroscopic studies of Ca^{2+}-binding proteins, Biochemistry 30 (1991) 9681–9686.
[67] M. Zhang, H. Fabian, H.H. Mantsch, H.J. Vogel, Isotope-edited Fourier transform infrared spectroscopy studies of calmodulin's interaction with its target peptides, Biochemistry 33 (1994) 10883–10888.
[68] T. Yuan, M.P. Walsh, C. Sutherland, H. Fabianm, H.J. Vogel, Calcium-dependent and independent interactions of the calmodulin-binding domain of cyclic nucleotide phosphodiesterase with calmodulin, Biochemistry 38 (1999) 1446–1455.
[69] A.A. Pandyra, A.P. Yamnick, V.V. Andrushchenko, H. Wieser, H.J. Vogel, Isotope-labeled vibrational circular dichroism studies of calmodulin and its interactions with ligands, Biopolymers 79 (2005) 231–237.
[70] E.M. Jones, T.C. Squier, C.A. Sacksteder, An altered mode of calcium coordination in methionine-oxidized calmodulin, Biophys. J. 95 (2008) 5268–5280.
[71] G. Wu, Z. Gao, A. Dong, S. Yu, Calcium-induced changes in calmodulin structural dynamics and thermodynamics, Int. J. Biol. Macromol. 50 (2012) 1011–1017.
[72] D. Sasakura, W. Nunomura, Y. Takakuwa, Dynamic secondary structural changes in Ca^{2+}-saturated calmodulin upon interaction with the antagonist, W-7, Biochem. Biophys. Res. Commun. 423 (2012) 360–365.
[73] S. Ebashi, M. Endo, I. Ohtsuki, in: E. Carafoli, C.B. Klee (Eds.), Calcium as a Cellular Regulator, Oxford Univ. Press, New York, 1999, pp. 579–595.
[74] A.S. Zot, J.D. Potter, Structural aspects of troponin–tropomyosin regulation of skeletal muscle contraction, Annu. Rev. Biophys. Chem. 16 (1987) 535–539.
[75] J.H. Collins, J.D. Potter, M.J. Horn, G. Wilshire, N. Jackman, The amino acid sequence of rabbit skeletal muscle troponin C: gene replication and homology with calcium-binding proteins from carp and hake muscle, FEBS Lett. 36 (1973) 268–272.
[76] J.M. Wilkinson, Troponin C from rabbit slow skeletal and cardiac muscle is the product of a single gene, Eur. J. Biochem. 103 (1980) 179–188.
[77] J.P. van Eerd, K. Takahashi, Determination of the complete amino acid sequence of bovine cardiac troponin C, Biochemistry 15 (1976) 1171–1180.
[78] J.D. Potter, J. Gergely, The calcium and magnesium binding sites on troponin and their role in the regulation of myofibrillar adenosine triphosphatase, J. Biol. Chem. 250 (1975) 4628–4633.
[79] Y. Ogawa, Calcium binding to troponin C and troponin: effects of Mg^{2+}, ionic strength and pH, J. Biochem. 97 (1985) 1011–1023.
[80] S. Morimoto, The effect of Mg^{2+} on the Ca^{2+} binding to troponin C in rabbit fast skeletal myofibrils, Biochim. Biophys. Acta 1073 (1991) 336–340.
[81] S. Linse, S. Forsén, in: A.R. Means (Ed.), Calcium Regulation of Cellular Function, vol. 30, Raven Press, New York, 1995, pp. 89–152.
[82] J. Evenäs, A. Malmendal, S. Forsén, Calcium, Curr. Opin. Chem. Biol. 2 (1998) 293–302.
[83] W. Lehman, J.F. Head, P.W. Grant, The stoichiometry and location of troponin I- and troponin C-like proteins in the myofibril of the bay scallop, *Aequipecten irradians*, Biochem. J. 171 (1980) 413–418.
[84] T. Ojima, K. Nishita, Troponin from Akazara scallop striated adductor muscles, J. Biol. Chem. 261 (1986) 16749–16754.
[85] T. Ojima, K. Nishita, Akazara scallop troponin C: Ca^{2+}-induced conformational change and interaction with rabbit troponin subunits, Arch. Biochem. Biophys. 299 (1992) 344–349.
[86] O. Herzberg, M.N.G. James, Structure of the calcium regulatory muscle protein troponin-C at 2.8 Å resolution, Nature 313 (1985) 653–659.
[87] K.A. Satyshur, S.T. Rao, D. Pyzalska, W. Drendel, M. Greaser, M. Sundarlingam, Refined structure of chicken skeletal muscle troponin C in the two-calcium state at 2 Å resolution, J. Biol. Chem. 263 (1988) 16620–16628.
[88] F. Yumoto, K. Nagata, Y. Miyauchi, T. Ojima, H. Tanaka, K. Nishita, I. Ohtsuki, M. Tanokura, Crystallization and preliminary X-ray analysis of the Ca^{2+}-bound C-terminal lobe of troponin C in complex with a troponin I-derived peptide fragment from Akazara scallop, Acta Crystallogr. F63 (2007) 535–537.
[89] Y.S. Kato, F. Yumoto, H. Tanaka, T. Miyakawa, Y. Miyauchi, D. Takeshita, Y. Sawano, T. Ojima, I. Ohtsuki, and M. Tanokura, Structure of the Ca^{2+}-saturated C-terminal domain of scallop troponin C in complex with a troponin I fragment, Biol. Chem. (in press).
[90] A. Malmendal, J. Evenäs, E. Thulin, G.P. Gippert, T. Drakenberg, S. Forsén, When size is important. Accommodation of magnesium in a calcium binding regulatory domain, J. Biol. Chem. 273 (1998) 28994–29001.
[91] F. Yumoto, K. Nagata, K. Adachi, N. Nemoto, T. Ojima, K. Nishita, I. Ohtsuki, M. Tanokura, NMR structural study of troponin CC-domain complexed with troponin I fragment from scallop striated muscle in solution, Adv. Exp. Med. Biol. 538 (2003) 195–201.
[92] R.E. Reid, J. Gariepy, A.K. Saund, R.S. Hodges, Calcium-induced protein folding, J. Biol. Chem. 256 (1981) 2742–2751.
[93] B.J. Marsden, R.S. Hodges, B.D. Sykes, A ^1H NMR determination of the solution conformation of a synthetic peptide analogue of calcium-binding site III of rabbit skeletal troponin C, Biochemistry 28 (1989) 8839–8847.
[94] G.S. Shaw, R.S. Hodges, B.D. Sykes, Probing the relationship between a-helix formation and calcium affinity in troponin C: ^1H NMR studies of calcium binding to synthetic and variant site III helix–loop–helix peptides, Biochemistry 30 (1991) 8339–8347.
[95] G.S. Shaw, in: H.J. Hans (Ed.), Methods in Molecular Biology, vol. 173, Humana, Totowa, NJ, 2001, pp. 175–181.
[96] T. Ojima, M. Maita, A. Inoue, K. Nishita, Bacterial expression, purification, and characterization of akazara scallop troponin C, Fish. Sci. 63 (1997) 137–141.